

ULTRAVIOLET TO NEAR-INFRARED k -SPECTRA MODELING OF SYNTHETIC LUNAR PYROCLASTIC GLASS. D. Trang¹, J. J. Gillis-Davis¹ and P. G. Lucey¹, ¹Hawai'i Institute of Geophysics and Planetology, University of Hawai'i at Mānoa, 1680 East-West Rd. POST602, Honolulu, HI, 96822 (dtrang@higp.hawaii.edu).

Introduction: The spectral character of lunar pyroclastic glasses in the ultraviolet (UV), visible (Vis), and near-infrared (NIR) is dependent on FeO and TiO₂ content [1]. On the basis of lab spectra of synthetic lunar glasses [2,3], we developed a spectral model that replicates UV-NIR absorptions due to these two major oxides. Next, this model is used to extract FeO and TiO₂ compositional information from spectral data of lunar pyroclastic deposits (e.g., Moon Mineralogy Mapper [4] and Spectral Profiler [5]) to yield distribution maps. Previously, FeO and TiO₂ algorithms of Lucey [6], were created to model the 1 μm absorption of olivine and pyroxene. Hence, their use to estimate the compositions of pyroclastic material was not intended.

Spectral Properties of Synthetic Glass: There are four dominant absorption features in synthetic glasses [7,8]. Similar to pyroxene NIR spectra, glass spectra exhibit two broad absorption features located at ~ 1 and ~ 2 μm , which are due to crystal field interactions of Fe²⁺ within their octahedral or tetrahedral sites respectively [7]. There are two additional absorptions in the UV-Vis wavelengths, ~ 0.34 and ~ 0.42 μm [8]. These bands are associated with Fe²⁺-Ti⁴⁺ intervalence charge transfer. Their interpretation is based upon observed relation between the absorptions and FeO and TiO₂ content in synthetic glasses [8].

The shape and location of the absorption features are dependent on the proportion of FeO and TiO₂. An increase in the FeO proportion will strengthen the 1 and 2 μm absorptions. These NIR absorption centers are constant regardless of FeO content [1]. As for the UV-Vis bands, the 0.34 and 0.42 μm absorptions strengthen and weaken depending on the proportions of FeO to TiO₂ [8]. Additionally, the 0.34 μm absorption will shift to longer wavelengths with increasing FeO and TiO₂ content [8,9]. Even with these observations of the UV-Vis bands, their properties as a function of FeO and/or TiO₂ are not well understood.

We use this additional information in the UV-Vis to construct more accurate FeO and TiO₂ distribution maps of pyroclastic deposits. These maps will reveal the global compositional diversity of pyroclastic deposits at high spatial resolution from recent missions.

Previous Work: A previous spectral model of lunar pyroclastic glass in the Vis-NIR has shown promising results [10]. Wilcox et al. [10] modeled the real (n) and complex (k) indices of refraction. They produced

a multi-linear function for n and k with respect to FeO and TiO₂ content at 98 wavelengths between 0.4-2.32 μm . To build on this earlier work, we model a larger spectral range that includes the UV and use the Modified Gaussian Model (MGM) to model the k -spectrum of synthetic glasses. MGM reduces the number of parameters needed to characterize a k -spectrum and allows the optical constants to be derived at any wavelength without need to resample the data [11,12]. Earlier uses of MGM have demonstrated the success on olivine and pyroxene k -spectra [e.g., 11,12,13,14,15].

Methods: We model the k -spectrum of seven synthetic lunar pyroclastic glasses with Gaussians in the UV-NIR. The composition of our synthetic samples ranged from ~ 0.5 wt.% (green glass) to ~ 15 wt.% (red glass) TiO₂ [2,3] with near constant FeO content (~ 20 wt.% FeO). The glasses were ground and sieved to < 53 μm . We assumed an average grain size of 45 μm , based upon analysis of green glass grain size [3].

The reflectance spectra of the synthetic glasses were acquired at the Reflectance Experiment LABoratory (RELAB). Measurements were performed at standard viewing geometries (i.e, 30° incidence, 0° emergence) with a spectral range of ~ 0.28 to 2.55 μm with sampling at every 0.01 μm [2,3]. Each reflectance spectrum was converted to k or single scattering albedo based upon the technique found in [16,17].

We fitted each k -spectrum of the synthetic glass with Gaussians. Specifically, the model consists of a linear function and four Gaussians. The linear function that models the continuum, is represented by:

$$C(\lambda) = y_{C1} + \left(\frac{y_{C2} - y_{C1}}{\lambda_{C2} - \lambda_{C1}} \right) \cdot (\lambda - \lambda_{C1}),$$

where (λ_{C1}, y_{C1}) and (λ_{C2}, y_{C2}) are the ordered pair (wavelength, k -value) needed to represent the function. The Gaussians model variations in k , and are represented by the equation:

$$g(\lambda) = s \cdot \exp \left(\frac{-(\lambda - \mu)^2}{2\sigma^2} \right),$$

where s is the strength, σ is the width, and μ is the center of the absorption. The four absorptions are located near ~ 0.34 , ~ 0.42 , ~ 1.0 , and ~ 2.0 . Since there are four Gaussians and a linear function, the k -spectrum of the synthetic glasses are determined with 14 parameters (three parameters for each Gaussian and two parameters from the linear function).

Each k -spectrum were fitted with an iterative fitting routine. The routine minimizes the mean absolute difference between the wavelengths of 0.3 to 2.55 μm by adjusting the four Gaussian centers, widths, and

strengths as well as the slope and intercept of the continuum.

Next, we produced a model that predicts the behavior of the fourteen-parameters as a function of FeO and TiO₂ content:

$$p(\text{FeO}, \text{TiO}_2) = A \cdot (\text{FeO}) + B(\text{TiO}_2) + C,$$

where A and B are constants. In particular, we used a multi-linear regression of the parameters against FeO and TiO₂, which in return produced the optical parameters.

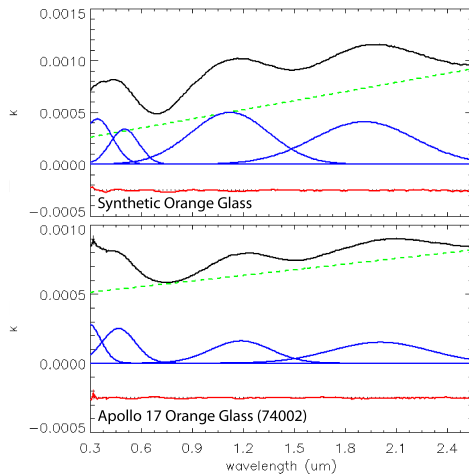


Figure 1: Model fits to synthetic orange glass (top) and lunar orange glass, 74002,339 (bottom). Black solid- k -spectrum; Green dotted-Continuum; Blue solid-Gaussians; Red-Residuals (data-model). Synthetic data appears similar to lunar pyroclastic glass.

Results and Discussion: We successfully fit each synthetic glass k -spectrum with Gaussians in the UV-NIR (**Fig. 1-top**). Also, we found that the regression of each parameter properly matches the model fit (**Fig. 2**). From the regression, we produced the fourteen optical parameters as a function of FeO and TiO₂ (**Table 1**).

Even though the regression matches the model fit, our initial results do not completely agree with theoretical results. For example, the optical parameters predict that the 1 and 2 μm absorption decreases with decreasing FeO content, which is not the case. This discrepancy may be due to the lack of variation of FeO content among our samples.

In addition to previous observation, we also noted the changes in absorption properties with respect to composition. For instance, increasing TiO₂ resulted into shifting the 0.42 μm absorption to longer wavelengths.

To test whether the same absorptions in the synthetic glasses are present in the actual lunar glass samples, we ran our iterative routine to lunar glasses (e.g., 74002,339 [18]). We found that both bands in the UV-Vis are needed to model the spectra of lunar glasses from the UV-NIR (**Fig. 1-bottom**).

Future Work and Conclusion: This model can reproduce any k -spectra of various FeO and TiO₂ content from 0.3 to 2.55 μm . However, this model does not completely agree with previous observations (e.g., relationship between FeO content and absorption strengths). This issue can be remedied by synthesizing more glasses with various FeO content. Additionally, producing synthetic glasses with various TiO₂ contents as well will provide a better insight to the shape and location of the ultraviolet/visible absorptions as a function of FeO and TiO₂.

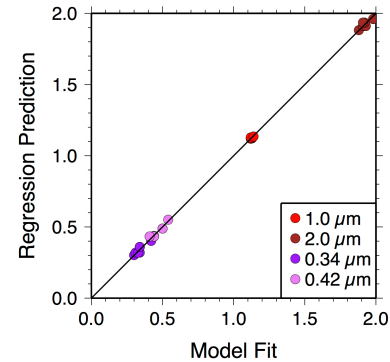


Figure 2: Comparison between absorptions centers of all four bands based upon the model fits to the predicted centers based upon the multi-linear regression. A good fit is when points are on the 1:1 line.

Table 1: Optical parameters of synthetic glasses.

Optical Parameter	A	B	Constant
1.0 μm center	-1.75E-03	1.50E-03	1.15E+00
1.0 μm strength	-8.97E-05	1.31E-05	2.36E-03
1.0 μm width	-1.40E-02	1.47E-03	5.23E-01
2.0 μm center	3.10E-03	4.65E-03	1.82E+00
2.0 μm strength	-7.35E-05	2.35E-05	1.83E-03
2.0 μm width	-1.52E-02	3.13E-03	5.90E-01
0.42 μm center	-1.96E-02	1.22E-02	8.14E-01
0.42 μm strength	-3.86E-05	2.27E-05	8.95E-04
0.42 μm width	4.88E-03	-5.12E-04	-2.29E-02
0.34 μm center	-6.68E-03	8.41E-03	4.28E-01
0.34 μm strength	-1.68E-04	2.08E-05	3.85E-03
0.34 μm width	1.44E-03	2.07E-03	2.56E-02
1.0 μm continuum	1.57E-04	-5.19E-06	-2.81E-03
2.0 μm continuum	2.17E-05	3.52E-05	1.28E-04

References: [1] Bell, P.M. and H.K. Mao (1972), *Proc. Lunar Sci. Conf. 3rd*, 545-553. [2] Gillis-Davis, J.J. et al. (2007), *LPSC XXXVIII*, Abs#1443. [3] Gillis-Davis, J.J. et al. (2008), *LPSC XXXIX*, Abs# 1535. [4] Pieters, C.M. et al. (2009) *Curr. Sci.*, 96(4), 500-505. [5] Ohtake, M. et al. (2008), *Earth Planets Space*, 60, 257-264. [6] Lucey, P.G. et al. (2000), *JGR*, 105(E8), 20,297-20,305. [7] Bell, P.M. et al. (1976), *Proc. Lunar Sci. Conf. 7th*, 2543-2559. [8] Wells, E. and B. Hapke (1977), *Science*, 195(4282), 977-979. [9] Loeffler et al. (1975), *Proc. Lunar Sci. Conf. 6th*, 2663-2676. [10] Wilcox, B.B. et al. (2006), *JGR*, 111, E09001. [11] Denevi, B.W. et al. (2007), *JGR*, 112, E05009. [12] Trang, D. et al. (submitted), *JGR*. [13] Sunshine, J.M. et al. (1990) *JGR*, 95(B5), 6955-6966. [14] Isaacson, P.J. et al. (2010), *Icarus*, 210(1), 8-13. [15] Klima, R.L. (2011), *MaPS*, 46(3), 379-395. [16] Hapke, B. (1993), *Theory of Reflectance and Emittance Spectroscopy*. Uni. of Cambridge, Cambridge. [17] Lucey, P.G. (1998), *JGR*, 103(E1), 1703-1713. [18] Pieters, C.M. and S. Tompkins (2005), *LPSC XXXVI*, Abs#1346.